ACR No. L4I27

NATIONAL ADVISORY COMMITTEE FOR AERONAUTICS

WARTIME REPORT

ORIGINALLY ISSUED
September 1944 as
Advance Confidential Report L4I27

CORRELATION OF FLIGHT DATA ON LIMIT PRESSURE COEFFICIENTS AND THEIR RELATION TO HIGH-SPEED BURBLING AND CRITICAL TAIL LOADS

By Richard V. Rhode

Langley Memorial Aeronautical Laboratory
Langley Field, Va.

WASHINGTON

NACA ACR No. L4I27

NATIONAL ADVISORY COMMITTEE FOR AERONAUTICS

ADVANCE CONFIDENTIAL REPORT

CORRELATION OF FLIGHT DATA ON LIMIT PRESSURE COEFFICIENTS AND THEIR RELATION TO HIGH-SPEED BURBLING AND CRITICAL TAIL LOADS

By Richard V. Rhode

SUMMARY

Flight data are presented to show that the absolute minimum or limit pressure coefficient on an airfoil is a function mainly of the Mach number for Mach numbers above about 0.3 and for usual flight values of the Reynolds number. The curve of limit pressure coefficient as a function of Mach number is established. The flight data also indicate the rate at which the pressure coefficient decreases with stream Mach number as the limit pressure is approached and when the local Mach number is greater than unity. Recent theoretical results of Garrick and Kaplan are modified and extrapolated in accordance with the flight data at the higher local Mach numbers to the established curve of limit pressure. A tentative working chart for the determination of the compressible-flow pressure distribution and of the lift coefficient beyond which potential flow cannot exist is thus established.

The lift coefficients at which potential flow ceases to exist (namely, the lift coefficients at the so-called compressibility burble) appear to be the actual maximum lift coefficients over a certain range of Mach number; that is, the lift coefficients corresponding to the attainment of limit pressure coefficient, as calculated by means of the tentative working chart for the P-47C-1 airplane, are in agreement with the maximum lift coefficients measured in abrupt pull-ups in the range of Mach number from 0.27 to 0.55.

Although the material presented does not permit deductions as to the relationship, if any, between the maximum lift coefficient and the limit pressure coefficient at the higher values of the Mach number, it seems

evident from published results of wind-tunnel tests and other data that at the higher Mach numbers the lift coefficients corresponding to limit pressure coefficient are not, in general, maximums but that they do define a boundary between two types of flow, one of which is turbulent or unsteady.

Certain practical implications of the results are discussed by means of applications to the V-n diagram. It is shown that modern fighter airplanes may stall over a considerable range of indicated speed at constant values of the load factor and that, in general, turbulent flow emanating from the wings may exist at almost any point on the V-n diagram within the operating range of altitude. From this result it follows that an important condition of tail loading occurs as a result of the superposition of buffeting load increments on maneuvering loads.

The deteriorating influence of skin wrinkles and bulges is also discussed and the necessity of designing smooth wings that do not bulge or wrinkle within the normal operating range of load factor is indicated.

INTRODUCTION

Because of the lack of a satisfactory theoretical solution of the high-speed stall or burble, limited flight tests were made on a P-47C-1 airplane for the purpose of obtaining data on the stall characteristics as a function of Mach number and Reynolds number. Stalled pull-ups were made at high altitude within conservative limits of load factor and measurements of acceleration, airspeed, and wing pressures were made. The data from these tests were needed because a number of recent tail failures were apparently caused by large loads resulting from premature stalling at moderately high speed and it was therefore necessary to establish some means of estimating the speeds and accelerations of stalling before a rational approach to the tail-load problem could even be attempted.

The results of the tests indicated large adverse compressibility effects on the maximum lift coefficient and verified the supposition that true stalls might occur at moderate values of lift and at moderately high

values of speed. The results could not be used to estimate the stalling conditions for other cases, however, and were not published.

Various investigators of the theoretical flow of compressible fluids have shown and experience indicates that serious flow disturbances do not take place upon the attainment at some locality of the speed of sound. The value of local Mach number or pressure coefficient beyond which potential irrotational flow can no longer exist has, however, remained elusive and speculative. Kaplan in reference 1 has indicated values of the limit pressure coefficient on the basis of a mathematical analysis of flow over a series of bumps. The results of reference 1 are most accurate for bumps of small thickness for which the values of the limiting pressure coefficient occur at rather high stream Mach numbers. For thick bumps, the analysis of reference 1 is less accurate and requires additional terms in the solution.

Since the tests were made on the P-47C-1 airplane, additional data have become available from tests on an XP-51 airplane and an S32C-1 airplane. The pressure measurements from these several tests and from an earlier test on an XF2A-2 airplane, together with the theoretical results of reference 1, are used to establish a useful working curve of limit pressure coefficient against Mach number.

In the present paper, the experimental curve of limit pressure coefficient is given. A tentative working chart is also presented for the solution of compressible flows in air to the limit pressure. This chart is based on a recent report by Garrick and Kaplan (reference 2) and has been adjusted and extrapolated at the higher local Mach numbers in accordance with the flight data.

Application of the results to the estimation of the limits on the V-n diagram at which burbling occurs is indicated and some implications of the results are discussed.

FLIGHT TESTS ON P-47C-1 AIRPLANE

Airplane maximum lift coefficient.- Abrupt pull-ups to stall were made at altitudes of 15,000, 20,000,

and 25,500 feet. Measurements were made of the normal component of acceleration and of the airspeed; the pressure altitudes were observed by the pilot. The airplane was weighed before take-off and allowance was made for fuel consumption up to the time of each pull-up to obtain correct values of wing loading for the purpose of computing the lift coefficient C_L. Accepted methods were employed in correcting the airspeed for compressibility effect.

The results of these tests are shown in figure 1 as maximum lift coefficient $C_{L_{max}}$ against stream Mach number M. There is no apparent effect attributable to differences of Reynolds number R; the value of $C_{L_{max}}$ at M = 0.4, where the data for two altitudes overlap, is virtually the same at Reynolds numbers of 9.8×10^6 and 13.4×10^6. The degradation in maximum lift with increasing Mach number is evident.

The nature of the acceleration records and the pilot's observation of the behavior of the airplane are of interest. Figure 2(a) shows a typical record for one of the pull-ups at 15,000 feet and figure 2(b) shows one at 25,500 feet. The sharp character of the break at maximum lift is apparent, particularly for the pull-up at 15,000 feet. In all of the pull-ups the breaks had the same sharp character, except in the one case noted in figure 1, the record for which is shown in figure 2(c); in this case the pilot reported a partial stall characterized by slight shuddering of the airplane.

The pilot's reports of the behavior of the airplane indicated that the stalls were, in general, symmetrical and "hard" - that is, there was little tendency to roll and the sudden change of force, both on the wing and on the tail, resulted in a hard shock to the airplane structure. In some cases the pilot noted shaking of the aileron.

Measurement of minimum pressure.- In addition to the measurements of $C_{L_{max}}$, a few pressures were measured in four of the runs to establish the minimum pressure, which was expected to occur near the nose of the wing. For this purpose seven closely grouped pressure orifices were installed at a section near the mid-semispan location, as shown in figure 3. Considerable

care was exercised to ensure a smooth surface and flush orifices, and high-frequency manometers were located in the gun compartment adjacent to the orifices to provide short pressure tubes and thus to minimize lag in the pressure measurements.

Because these tests were made during the course of another investigation on the airplane with which it was desired not to interfere and because of other limitations, the pressure investigation could not be as complete as desired. For these reasons, even with the orifice locations limited as stated, only one-half the orifices could be connected to the manometers at one time, so that the flight had to be repeated. Actually, an abrupt pull-up was made at 20,000 feet followed by a check pull-up with the same set of connections; the airplane was then brought to earth, connections changed, and the two pull-ups repeated within about 1/2 hour of the first pull-ups. The pull-ups were nearly identical, as indicated by the test points for the altitude of 20,000 feet shown in figure 1.

The minimum pressure coefficient measured at the nose in these tests was -5.55 and the Mach number was 0.42. The minimum pressure occurred at the time of maximum lift; this feature of the result is shown in figure 4 by the time histories of pressure coefficient and normal acceleration, in which the occurrence of stall is indicated by the sharp break and the subsequent irregularity in the acceleration curve.

FLIGHT TESTS ON XP-51 AIRPLANE

Available results from flight tests on the XP-51 airplane include pressure measurements obtained in a stalled pull-up at a Mach number of 0.445 and in three pull-outs from dives at Mach numbers of about 0.73.

The pressures were measured around the profile at three stations along the span of the left wing. The spacing of the orifices at the nose, in general, was not so close as in the case of the P-47C-1 airplane and the connecting tubes to the manometer in the fuselage were longer. The minimum pressure coefficient actually measured was -4.60 at the nose of the inboard station, and this value occurred at a Mach number of 0.445.

The minimum pressure coefficient measured at the nose of the middle station was -4.25 at a Mach number of 0.445. The minimum pressures for both the root and the middle station occurred somewhat later than the maximum lift coefficient or acceleration. Figure 5 shows for the midsection the time history of the pressure coefficient at the point at which the minimum pressure occurred, together with the time history of the normal acceleration. At the instant of maximum lift, the minimum pressure coefficient measured was -4.01 and the Mach number was 0.455. It appears that, as in the case of the P-47C-1 airplane, the maximum lift coefficient occurred substantially in conjunction with the attainment of a limit value of minimum pressure coefficient, with the exception that the minimum pressure coefficient continued to persist for a period of time following the occurrence of the stall. The pressure distribution over the upper surface of the middle station, at which the nose orifices were the most closely spaced, is shown in figure 6 for the instant of maximum lift.

An example of the behavior of the minimum pressure coefficient in the dive pull-outs is shown in figure 7, in which the lift coefficient, minimum pressure coefficient, and stream Mach number are plotted against time. It is seen that, before the pull-out started, the minimum pressure coefficient decreased as the Mach number increased to a value that subsequently remained nearly constant for a time. As the lift coefficient was sharply increased from about 0.1 to about 0.4, however, the minimum pressure coefficient failed to respond in a manner that would have been expected for low values of the Mach number. In fact, the singular constancy of the pressure coefficient in this case suggests the attainment of a limit value for the Mach number shown.

The apparent attainment of limit values of the minimum pressure coefficient in the dive pull-outs was not related to any obvious stall, although the pressure records showed that turbulent flow existed behind, but not ahead of, the location where the limit pressure occurred.

FLIGHT TESTS ON SB2C-1 AIRPLANE

In the course of an investigation of the flight loads on an SB2C-1 airplane, pressures were measured

along the chord at three spanwise stations on the left wing. Although the tests were not carried to very high Mach numbers or lift coefficients, a series of pull-outs was made up to a Mach number of 0.645 and a lift coefficient of 0.45. In the last pull-out, as contrasted with previous ones of lower speed and acceleration, there were definite evidences of disturbance to flow over the wing and of separation from the upper surface. These evidences included sudden losses in total pressure in a region extending from 3 inches to 6 inches above the trailing edge of the wing and discontinuity in the curve of wing bending moment against wing lift. Moreover, as for the XP-51 airplane, the minimum pressure coefficients showed a tendency to stay at a nearly constant value over a period of time during which the normal acceleration of the airplane increased and decreased. Although the indications were not so sharply defined for the SB2C-1 airplane as for the P-47C-1 and XP-51 airplanes, it is believed that a limit value of pressure coefficient had been obtained and that, associated with its occurrence, separation of flow occurred over the upper surface of the wing. In this case the minimum pressure coefficient was -2.15 and occurred at a Mach number of 0.645.

LIMIT PRESSURE COEFFICIENT

It seems evident that, in each of the flight tests cited, the minimum pressure coefficient measured at any point along the chord attained a limit value at which separation of flow or turbulence occurred. The several values of minimum pressure coefficient measured in the flight tests cited herein are plotted against Mach number in figure 8. The point shown for the stalled pull-up of the XP-51 airplane is that for the nose of the root station. This point was chosen because it was the minimum of all values measured and is probably the most accurate value considering the effects of lag in the tubes connecting the orifices to the manometer. Also shown in figure 8 are results from reference 1 for bump thickness ratios up to about 8 percent and a point from tests of the XF2A-2 airplane reported in reference 3. This last point was taken from the original data, not from the cross-faired pressure plots shown in reference 3.

The manner in which the various points fall along a single curve in figure 8 notwithstanding differences in airfoil section, lift coefficient, and Reynolds number seems to verify the real existence of a limit pressure coefficient dependent mainly upon Mach number and to establish the curve as the definition of this limit pressure coefficient as a function of the Mach number.

MODIFICATION AND EXTRAPOLATION OF THEORETICAL FLOW

Figure 8 shows, in addition to the experimental values of limit pressure coefficient, the theoretical values of pressure coefficient in compressible flow presented in reference 2. The sonic curve shown in figure 8 represents the locus of points at which the local Mach number is unity. The theoretical results indicate that the negative pressure coefficients may continue to decrease in a continuous manner with increase in the stream Mach number to values corresponding to a constant local Mach number which, for a particular velocity correction formula given in reference 2, has the value 1.15. The theoretical results, however, do not extend to the experimental curve of limit pressure coefficient and, in order to effect solutions of the flow to this limit, the theoretical flow must be extrapolated. Also, the theoretical curves as extrapolated must be examined in consideration of the available flight data to ensure that solutions in reasonable agreement with the flight results are obtained.

In order to effect an extrapolation that would conform to the desirable condition of agreement with the flight data, three steps were taken. First, the pressure distribution obtained immediately prior to the stall of the XP-51 airplane was compared with the calculated pressure distribution as corrected for compressibility by the use of the Garrick-Kaplan curves directly extrapolated; the disagreement in the two results was then used as a guide to effect a modified extrapolation. Because this first step serves as a guide to extrapolation only in the region of the greater numerical values of the negative pressure coefficient, a second step, aimed at extrapolation in the region of the lower values, was to examine the rate at which the

minimum pressure coefficient changed with Mach number just prior to the attainment of the limit pressure in the dives of the XP-51 airplane. The experimental rate was then used as a guide to the extrapolation. Finally, the modified and extrapolated flow curves, together with the established curve of limit pressure coefficient, were used to estimate the probable maximum lift coefficients of the P-47C-1 airplane over a range of Mach number and these lift coefficients were checked against those obtained experimentally by means of the accelerometer and airspeed measurements.

Figures 6 and 8 show the results of the first step. In this step only the negative pressure coefficients were considered and, because of the presence of the flap and other irregularities in the wing near the trailing edge, attention was focused on the forward half of the wing, where the smoothest flow existed. Furthermore, the comparisons were effected by matching the peak pressure coefficients at the nose and observing the degree of agreement in the pressure curves as they extended back toward the trailing edge. For this purpose, the minimum pressure coefficient occurring at the nose of the airfoil was assumed to be -4.60 instead of the measured value of -4.01, which occurred at the time of maximum lift. This value was chosen because of the probability that the minimum pressure coefficient actually occurred somewhere between the points at which pressure orifices were located. It may be noted that -4.6 is the value found on the curve of limit pressure coefficient in figure 8 for a Mach number of 0.455 at which the maximum lift occurred. Figures 6 and 8 indicate that better agreement between the calculated and measured pressure distributions is obtained with a compressibility correction that bends up less steeply than the Garrick-Kaplan curves in the region of and beyond the sonic curve. Below the sonic curve, the curve of best agreement lies between the approximate result of von Kármán (reference 4) and the particular case discussed in reference 2. In fact, the experimental curve follows very closely the Temple-Yarwood approximation reported in reference 5 and discussed in reference 2.

The result of the second step is shown in figure 8 as a plot of the simultaneous values of minimum pressure coefficient and stream Mach number shown in the time history of figure 7 prior to the pull-out.

Although the angle of attack did not change sufficiently during the dive to affect the significance of this result, a bulge in the upper surface of the wing grew larger with increasing speed so that the profile did not remain quite constant. At the higher speed, just before the pull-out, the location of minimum pressure shifted from about 42 percent to 50 percent chord, which was the location of the crest of the bulge. The plot of pressure coefficient in figure 8 is that of the minimum pressure coefficient regardless of location and is the most significant possible representation of the behavior of the pressure coefficient with increasing Mach number. The result shown therefore is a substantially true indication for the present purpose and serves as a legitimate guide to the extrapolation. Again, it appears that the experimental flow curve bends up less steeply than the Garrick-Kaplan curve. The experimental curve here is somewhat more steep than the Temple-Yarwood approximation.

Figure 9 is a complete flow chart based primarily on the Garrick-Kaplan results modified and extrapolated in accordance with the experimental results as indicated. The Temple-Yarwood approximation was used to some extent to assist in systematizing the upper parts of the flow curves. This chart may be regarded as a tentative working chart for the solution of the pressure distribution to the limit pressure and of the lift coefficient at which marked changes in flow occur. No doubt some slight modification of the chart will prove desirable as additional flight data become available or can be analyzed.

It may be pointed out that, whereas the particular velocity correction formula discussed in reference 2 yields a limit curve for which the local Mach number is 1.15, the Temple-Yarwood approximation yields a limit curve for which the local Mach number is 1.35 calculated according to the method of reference 2. The experimental curve corresponds to a local Mach number of about 1.5 at the intermediate and high values of the minimum pressure coefficient and to somewhat lower local Mach numbers at the lower values of pressure coefficient. Apparently, then, no one velocity correction formula would apply over the entire range of conditions and it appears from the present experimental results that the limit curve of figure 9 is probably the one applicable to modern airplanes.

COMPARISON OF ESTIMATED AND MEASURED "LIMIT LIFT COEFFICIENTS"

Pressure distributions for three sections of the wing of the P-47C-1 airplane were calculated for incompressible flow at several lift coefficients according to the method of reference 6. The sections for which the calculations were made were taken at stations near the root, midway between the root and tip, and near the tip. In each case care was taken to ensure accurate evaluation of the peak pressure near the nose. These pressure distributions were expanded to various Mach numbers through the use of figure 9 until the limit pressure coefficient was attained. The new lift coefficients were then found by mechanical integration. In this way the "limit lift coefficients" were obtained as a function of free-stream Mach number.

The span load distribution was then determined according to the method of reference 7 and the section lift coefficients were plotted against wing lift coefficient. Since there was no reason to believe that the span load distribution would be greatly affected by compressibility until a breakdown in flow occurred at some station, no serious attempt was made to correct this distribution for compressibility. Because the wing has some twist, however, the well-known Glauert factor $\frac{1}{\sqrt{1 - M^2}}$ was applied for a Mach number of 0.55 (a value near the upper limit attained in the tests on the P-47C-1 airplane) to indicate approximately the degree to which the ultimate result might be affected by such a correction. The uncorrected and corrected values are shown in figure 10.

Finally, the section values of limit lift coefficient, as previously determined for several values of the Mach number, were located in the plot of section lift coefficient against wing lift coefficient. (See fig. 10.)

Figure 10 shows at a glance approximately where the change in flow may be expected to occur first along the span. At the lower Mach numbers and higher lift coefficients, the high pressure coefficients at

the relatively sharp nose of the thin tip section result in earlier change near the tip. At the higher Mach numbers and lower lift coefficients, the greater thickness of the root section causes the flow to break down first at the inboard location. The initial occurrence of some breakdown in flow over a narrow region along the span does not mean, however, that a change of lift of the whole wing will be manifested at the same time.

It is evident that the lift of the wing at which a change in flow is likely to be manifested by some noticable change in behavior of the airplane will lie between the values corresponding to the limit lifts of the root and tip sections. Without knowledge of the rate at which the lift changes beyond the critical value at each station, the wing lift coefficient of course cannot be exactly determined. As an approximation, however, a mean wing lift coefficient may be determined by weighting the values corresponding to the critical section coefficients according to the chords of the sections. The wing lift coefficients determined in this manner for the P-47C-1 airplane are shown in figure 10. Figure 11 shows the mean wing lift coefficients plotted against Mach number. Also shown for comparison are the experimental values of maximum lift coefficient from figure 1, corrected for the upward-acting tail load to represent more nearly the maximum lift coefficient of the wing alone. The agreement between the experimental maximum lift coefficients and the limit lift coefficients as estimated from the chart of figure 9 serves both as a practical check of the chart and as an indication that the breakdown of flow associated with the attainment of the limit pressure coefficient defines the maximum lift coefficient for the wing of the P-47C-1 airplane within the test range of Mach number.

DISCUSSION

Applications to V-n Diagram and Implications Relative to Tail Loads

In order to illustrate some practical implications of the foregoing results, V-n diagrams (fig. 12) have been prepared for the P-47C-1 airplane. The V-n diagram

is simply a graphical representation of the general lift equation, where the lift L is given in terms of the airplane weight W, as follows:

$$n = \frac{L}{W}$$

$$= \frac{C_L \frac{1}{2}\rho V^2}{W/S}$$

where

ρ mass density of air

V true airspeed

S wing area

The curved boundaries shown in figure 12 are the limits defined by the estimated values of lift coefficient at the limit pressure coefficient and hence apply to the wing only; airplane load factors are about 5 or 6 percent higher than the limits shown owing to the upward-acting tail load. The mean line through the acceleration values measured at 25,500 feet and corrected for tail load is also shown for comparison.

This V-n diagram shows at a glance the values of acceleration and $V\sigma^{1/2}$ at which breakdown of flow or burbling occurs at any altitude. A point of interest is that the lines of constant lift coefficient are also lines of constant Mach number when considered as connecting the V-n boundaries for the different altitudes.

It may be noted that there is a region of altitude and speed at which burbling occurs with high load factors in the neighborhood of the limit load factors for which modern fighter and pursuit airplanes are designed. For example, if a horizontal line is drawn on the diagram at $n = 8$, this line intersects the sea-level boundary at about 285 miles per hour and at 520 miles per hour. Burbling can therefore occur at sea level at either of these two speeds. As the altitude increases, the lower speed at which burbling occurs at 8g increases and the

higher speed decreases until, at about 8000 feet, the flow breaks down at 8 g at a single speed of about 370 miles per hour; at other speeds, burbling already has occurred at lower load factors. Thus, if pull-outs or pull-ups are carried out to 8 g between sea level and 8000 feet, burbling may be expected to occur at any speed, depending upon the altitude, between the sea-level limits of 230 miles per hour and 530 miles per hour. Similar conditions obtain, with different limits of speed and altitude, for other values of acceleration.

The effect of wing loading is indicated by a comparison of figure 12, which applies for a wing loading of 40 pounds per square foot, and figure 13, which applies for a wing loading of 30 pounds per square foot. The boundaries for equal altitudes move to higher values of acceleration as the wing loading decreases or, by putting it conversely, burbling occurs at given values of acceleration and lift coefficient at higher altitude as the wing loading decreases. In the case under consideration, the effect of decreasing the wing loading from 40 pounds per square foot to 30 pounds per square foot has been to increase the altitude at which burbling occurs at a single speed at 3g from about 8000 feet to about 15,000 feet.

These results lead to the conclusion that breakdown of flow from the wings of modern fighter airplanes may occur as a result of compressibility effects over most of the area of the V-n diagram, the accelerations and speeds depending upon the wing loading and altitude for any given airplane geometry. Moreover, within the usual range of wing loading, such breakdown may occur in the vicinity of the limit load factor within the normal operating range of altitude and speed. This fact, of course, has an important bearing on the loads imposed on the airplane structure, especially that of the tail. In the case of the horizontal tail, the existence of the high load factor signifies, in general, a large upward-acting tail load; when the flow breaks down over the wing while the quasi-static load on the tail is large, a critical condition is likely to occur because of the superposition of additional load increments. These load increments include those resulting from buffeting (see reference 8) and those resulting from changes in the location of the aerodynamic center of the wing. Furthermore, if the breakdown in flow is unsymmetrical over the wings, rolling and yawing may be

expected to occur and unsymmetrical components of tail load will be imposed. If the breakdown in flow is a true stall, as the evidence indicates will be the case at the more moderate values of the Mach number, and if some aileron or rudder has been applied, a snap roll may ensue with very large yaw angles and large unsymmetrical tail-load components. In this case, too, the loads on the vertical tail surfaces may be critical because of the occurrence of a very large yaw angle at high speed.

Although reduction of wing loading increases the altitude at which the high loads occur, the probability of stalling or burbling still remains within the range of usual operating conditions for all commonly used wing loadings. On the other hand, the range of altitude within which stalling or burbling does not occur over a considerable range of speed is greatly increased with reduced wing loading so that, in general, the lighter the wing loading the less probable is the occurrence of change of flow, especially at the higher values of load factor. The lighter wing loadings are therefore advantageous in this respect.

Differentiation between Stalling and Burbling

Care has been exercised to avoid the use of the terms "stall" and "maximum lift" in this report except when the breakdown of flow at maximum lift or maximum lift was specifically meant. The results reported herein appear to indicate definitely enough that, when the limit pressure coefficient is reached at high to moderate values of the lift coefficient and at correspondingly low to moderate values of the Mach number, the breakdown in potential flow induces loss of lift and results in a turbulent wake of considerable strength. In other words, the limit pressure coefficient appears to define true maximum lift, or stalling, over a certain range of Mach number, the upper limit of which has not yet been established.

In the high-speed pull-outs of the XP-51 airplane at Mach numbers of about 0.74 and at lift coefficients of about 0.4, the mere attainment of the limit pressure coefficient did not result in any noteworthy manifestation of troublesome conditions although, as has previously been noted, the pressure records indicated the

existence of turbulence behind the location at which the limit pressure coefficient occurred. It is felt that the reason for the lack of noteworthy effects in this case may have been that the limit pressure coefficient occurred rather far back on the upper surface (see fig. 16) and that the turbulent wake was consequently narrow and missed the tail. Furthermore, the existence of a slight bulge in the profile at the location of the limit pressure may have stabilized the location of the shock and thus have led to the maintenance of relatively steady flow conditions.

That the attainment of the limit pressure coefficient in the pull-outs of the XP-51 airplane did not correspond to maximum lift is obvious from the data in figure 7, which show that the lift coefficient can change considerably while the minimum pressure coefficient remains nearly constant. The reason for this behavior is perhaps evident from figure 16. It may be observed that, since the limit pressure coefficient occurred at the 50-percent-chord station and pressure coefficients of much lower magnitude were present forward of this point, there is no bar to the further reduction of the pressures over the forward half of the wing until the limit value is attained there; that is, as the angle of attack is increased, the pressure diagram may continue to be "filled in" over the forward portion until the limit pressure is attained at the nose.

The determination of maximum lift at the higher values of the Mach number is therefore not settled by the material contained herein. There is no doubt that flight can be accomplished at the higher Mach numbers outside the boundaries of the V-n diagram established by the limit pressure, but the maximum possible load factors are not at present subject to analytical determination. On the other hand, there is also little or no doubt that at these higher Mach numbers the limit pressure does establish boundaries on the V-n diagram between two regimes of flow, one of which is turbulent or unsteady. Whether the change of flow and the turbulence introduce hazardous conditions depends upon, among other things, the geometry and dynamics of the airplane and the magnitude of the dynamic pressure.

Effect of Skin Bulging and Wrinkling

It should be reiterated at this point that the test results for the P-47C-1 airplane were obtained at sufficiently high altitude or at sufficiently low speed to ensure that the load factors would not be high. For this reason the wing was not stressed sufficiently to cause serious distortion of the wing profile due to bulging or wrinkling of the skin, and the results therefore apply to the undistorted profile. The V-n diagrams shown herein also apply to the undistorted profile.

It is easy to show, however, that distortions of the profile have a substantial deleterious effect upon the lift coefficient at which the limit pressure occurs. This fact is almost self-evident but is illustrated by figures 14 and 15. Figure 14 shows the upper surface of an airplane wing under static test at a load factor of 8. The report of the test indicates that the wrinkles started to form at a load factor of 6 when the wing was first loaded and at a load factor of 4 when the wing was reloaded after having been loaded to the design yield load. Figure 15 shows the calculated incompressible-flow pressure distribution for the forward portion of the upper surface of this wing at two values of the section lift coefficient. The figure also shows the pressure distribution as modified by the presence of a wrinkle having dimensions such as those shown in figure 14. The modification of the pressure distribution as caused by the wrinkle was calculated by the method given in reference 9. Referring these pressure distributions to figure 9 shows that the presence of the wrinkle seriously decreases either the lift coefficient at a given value of the Mach number or the Mach number at a given value of the lift coefficient at which the limit pressure coefficient is reached.

The flatter types of pressure distribution associated with the newer types of airfoil at the lower lift coefficients may be sensitive to slight distortions of the profile as the limit pressure is approached. Measurements of the profile distortion at the mid-semispan location on the XP-51 airplane, for example, indicated that the crest of a wide bulge occurred on the upper surface at the 50-percent-chord station. The height of the bulge was about 0.2 percent chord. Elsewhere along the chord the heights of the bulges were

only about one-twentieth that magnitude. It might be expected that the effect of the bulge would be to modify the incompressible-flow pressure diagram in a manner similar to that illustrated for the wrinkle in figure 15; of course, the pressure increments would be less drastic than for the wrinkle (the height of which, incidentally, was 0.4 percent chord) and, since the bulge was wider than the wrinkle, the pressure increments would be spread over a somewhat greater distance along the chord.

Figure 16 shows the estimated pressure distribution for the undistorted upper-surface profile together with the pressure distribution actually measured just as the limit pressure was reached. Although the point has not been verified, it appears possible that the effect of the bulge in the upper surface was to shift the position at which the region of low pressure occurred and also to cause the pressure to decrease to the limit value.

Bulging and wrinkling of the skin appear, therefore, to have two important effects. First, as wrinkling occurs at the higher load factors, the lift coefficients of burbling are reduced and the actual V-n boundaries for the lower altitudes may have flatter and lower crests than illustrated by the examples shown for an undistorted wing in figures 12 and 13. Second, the existence of bulging and wrinkling makes very difficult, if not practically impossible, the prediction of an exact pressure distribution at the higher loads and speeds. It would seem, therefore, that every effort should be made to design the wings of high-performance airplanes to have rigid shells rather than to permit wrinkling and bulging of the skins. It is equally evident, of course, that other flow deteriorating influences on the wing profile should be suppressed to the vanishing point.

Langley Memorial Aeronautical Laboratory
National Advisory Committee for Aeronautics
Langley Field, Va.

REFERENCES

1. Kaplan, Carl: The Flow of a Compressible Fluid past a Curved Surface. NACA ARR No. 3K02, 1943.

2. Garrick, I. E., and Kaplan, Carl: On the Flow of a Compressible Fluid by the Hodograph Method. I - Unification and Extension of Present-Day Results. NACA ACR No. L4C24, 1944.

3. Rhode, Richard V., and Pearson, H. A.: Observations of Compressibility Phenomena in Flight. NACA ACR No. 3D15, 1943.

4. von Kármán, Th.: Compressibility Effects in Aerodynamics. Jour. Aero. Sci., vol. 8, no. 9, July 1941, pp. 337-356.

5. Temple, G., and Yarwood, J.: The Approximate Solution of the Hodograph Equations for Compressible Flow. Rep. No. S.M.E. 3201, R.A.E., June 1942.

6. Theodorsen, T., and Garrick, I. E.: General Potential Theory of Arbitrary Wing Sections. NACA Rep. No. 452, 1933.

7. Anon.: Spanwise Air-Load Distribution. ANC-1(1), Army-Navy-Commerce Committee on Aircraft Requirements. U.S. Govt. Printing Office, April 1938.

8. Flight Research Maneuvers Section: Flight Studies of the Horizontal-Tail Loads Experienced by a Modern Pursuit Airplane in Abrupt Maneuvers. NACA ARR No. L4F05, 1944.

9. Jones, Robert T., and Cohen, Doris: A Graphical Method of Determining Pressure Distribution in Two-Dimensional Flow. NACA Rep. No. 722, 1941.

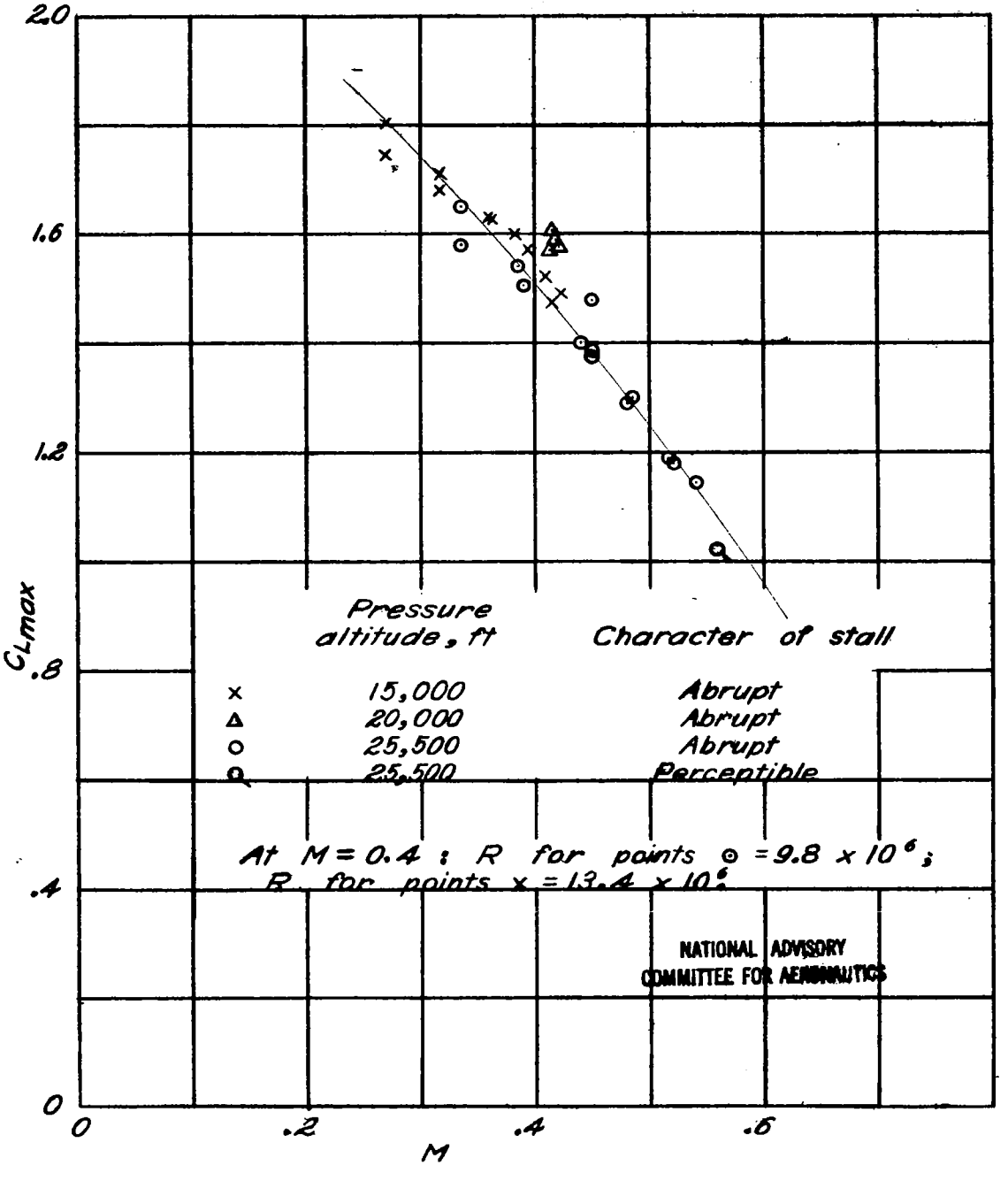

Figure 1.- Maximum lift coefficient of P-47C-1 airplane in abrupt pull-ups.

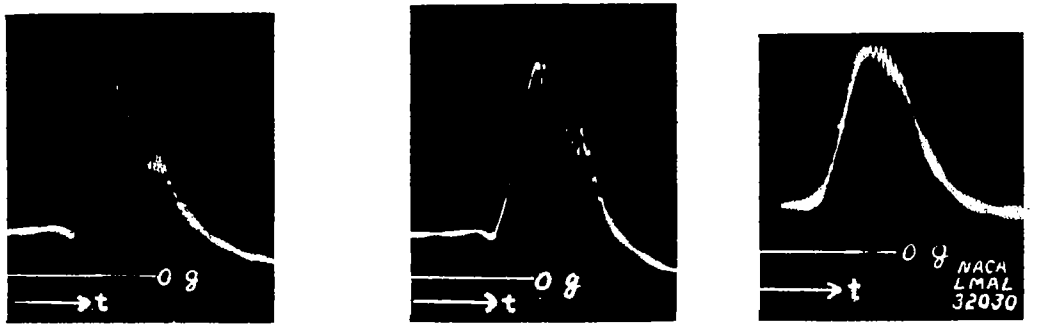

(a) At 15,000 feet; abrupt stall.

(b) At 25,500 feet; abrupt stall.

(c) At 25,500 feet; perceptible stall.

Figure 2.- Acceleration records taken on P-47C-1 airplane during abrupt pull-ups.

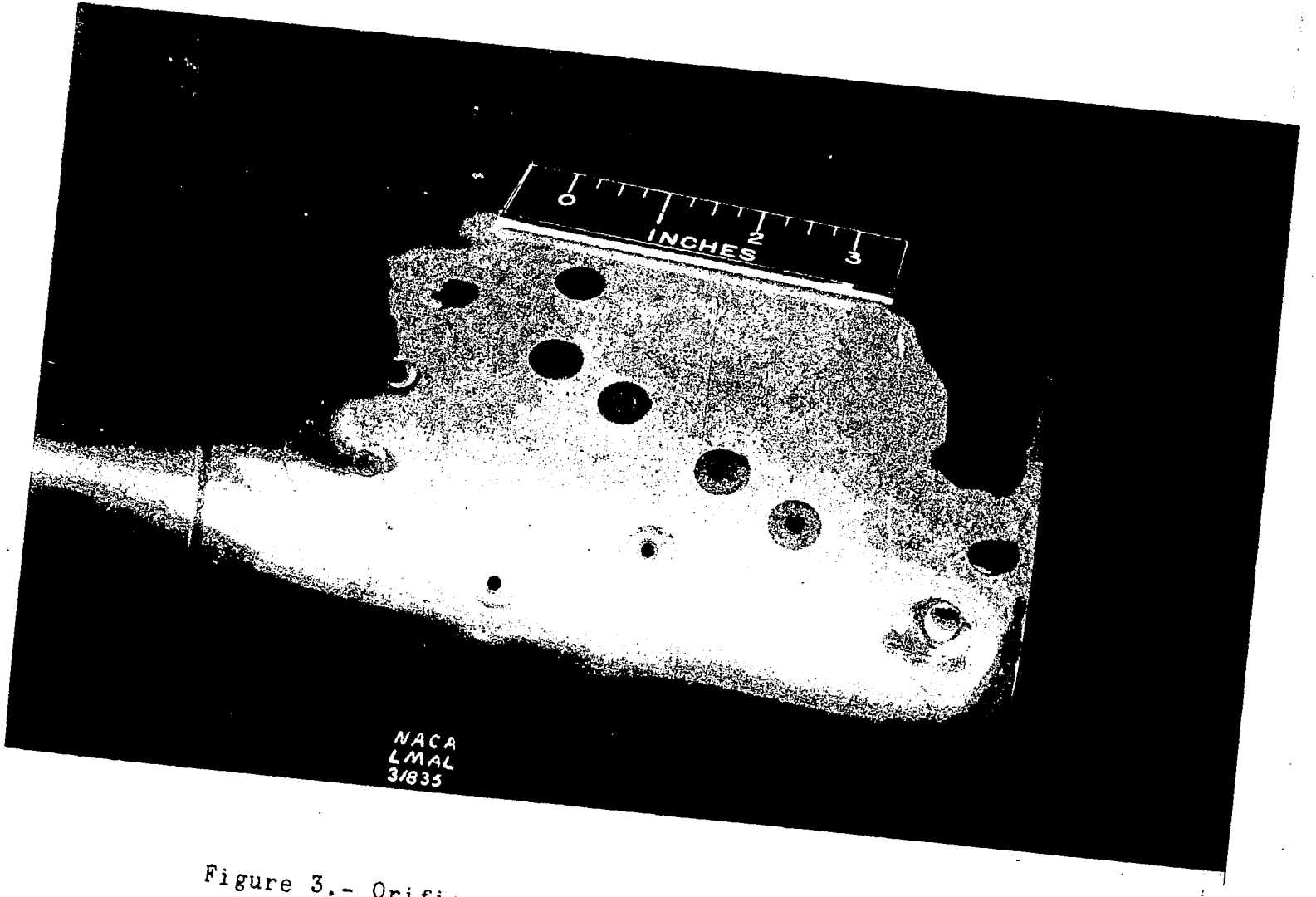

Figure 3.- Orifices in nose of wing on P-47C-1 airplane.

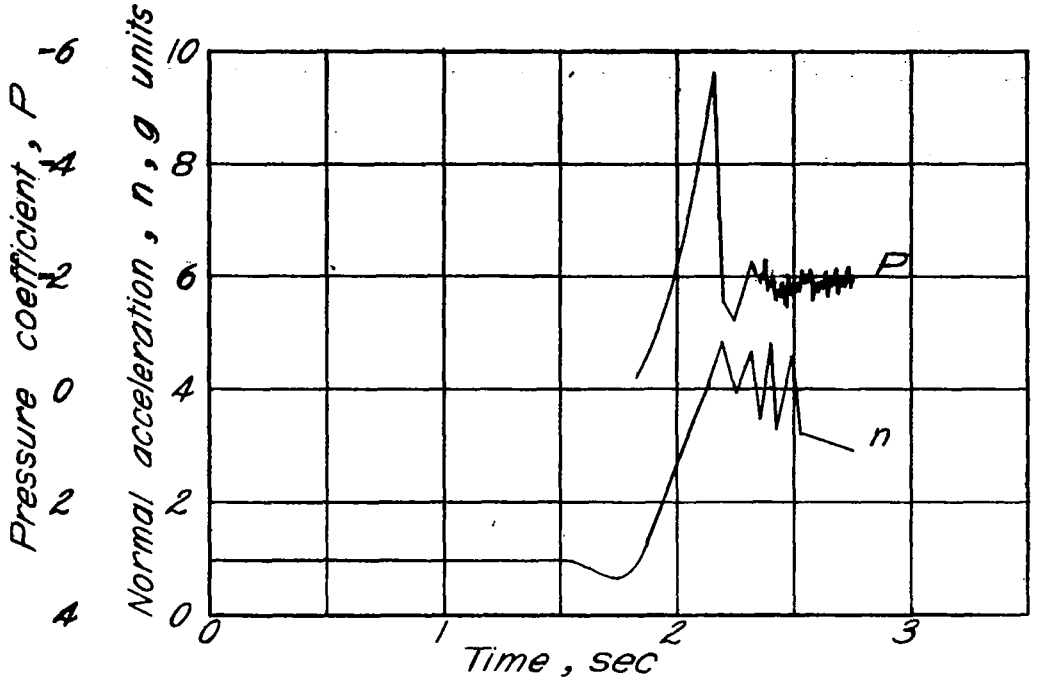

Figure 4.- Time histories of normal acceleration and of minimum pressure on nose of midsection of wing in abrupt stalled pull-up of P-47C-1 airplane.

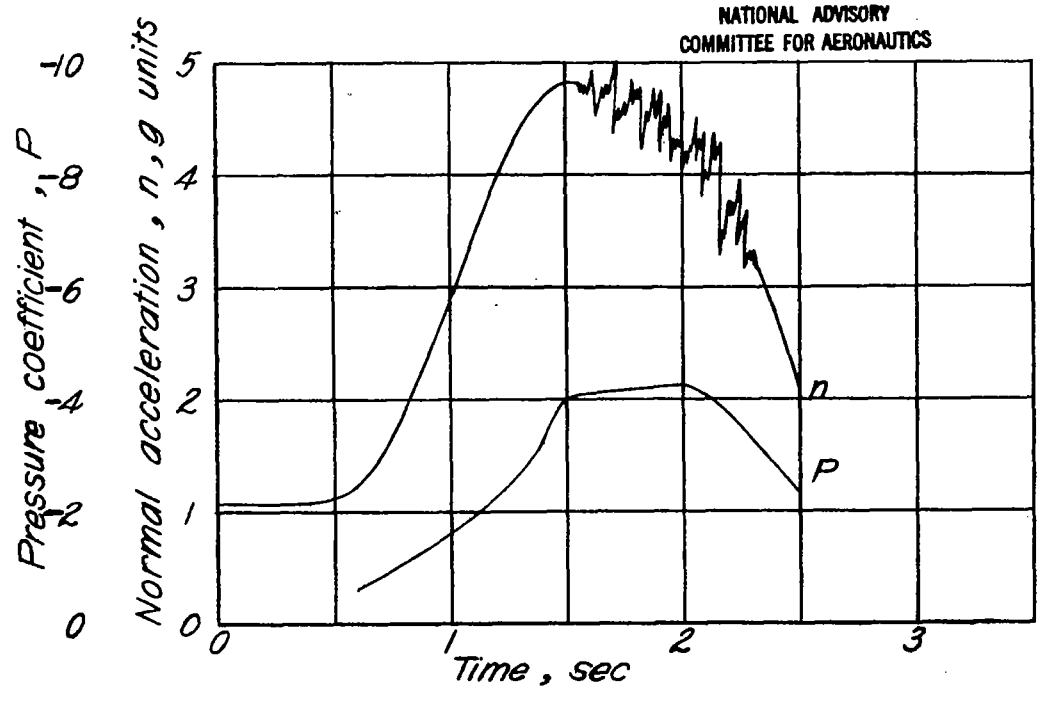

Figure 5.- Time histories of normal acceleration and of minimum pressure on nose of midsection of wing in stalled pull-up of XP-51 airplane.

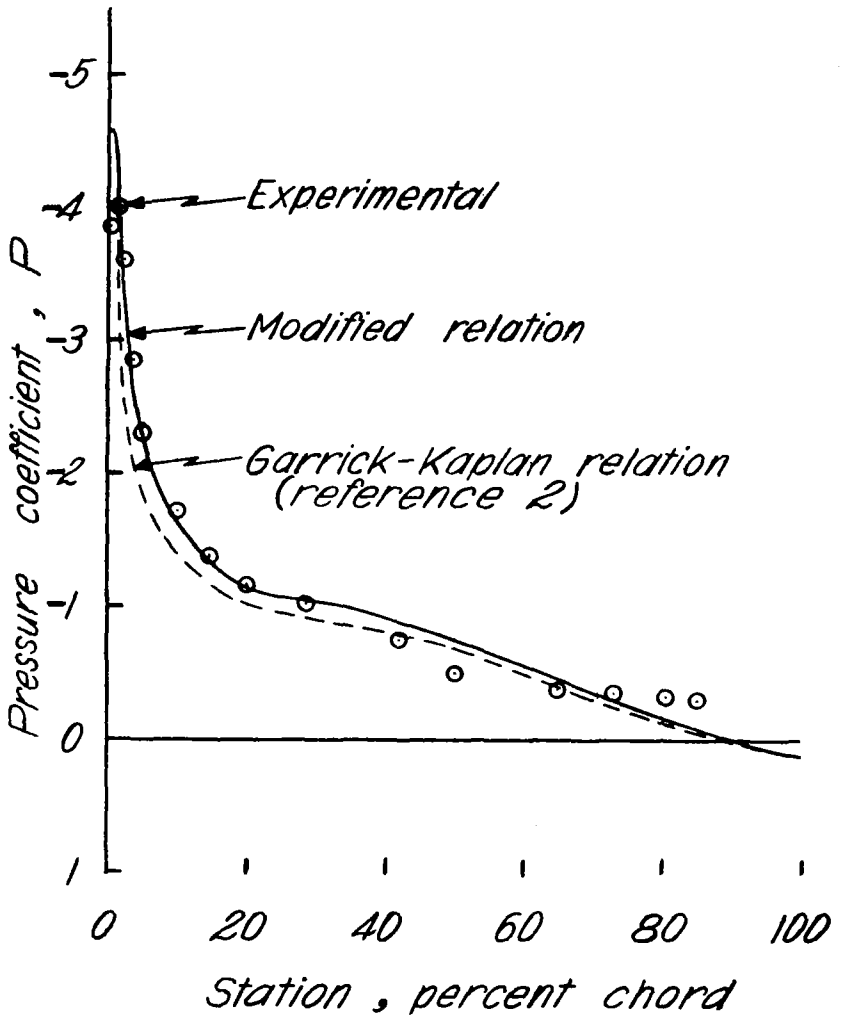

NATIONAL ADVISORY
COMMITTEE FOR AERONAUTICS

Figure 6.- Pressure distribution over upper surface of wing of XP-51 airplane at maximum lift compared with estimated distributions based on extrapolated Garrick-Kaplan relation and on modified relation.

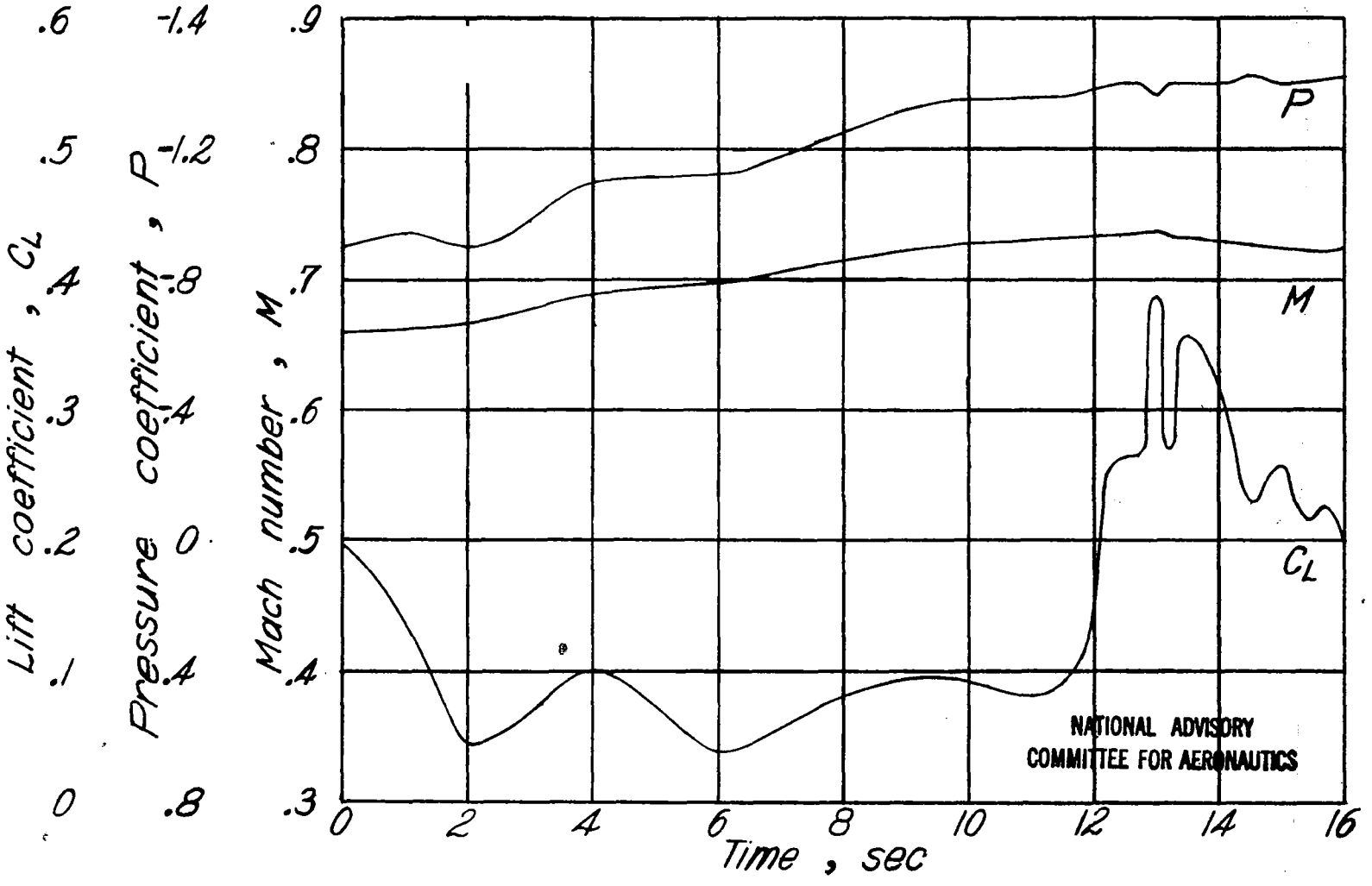

Figure 7.- Time history of minimum pressure coefficient on midsection of wing of XP-51 airplane in pull-out.

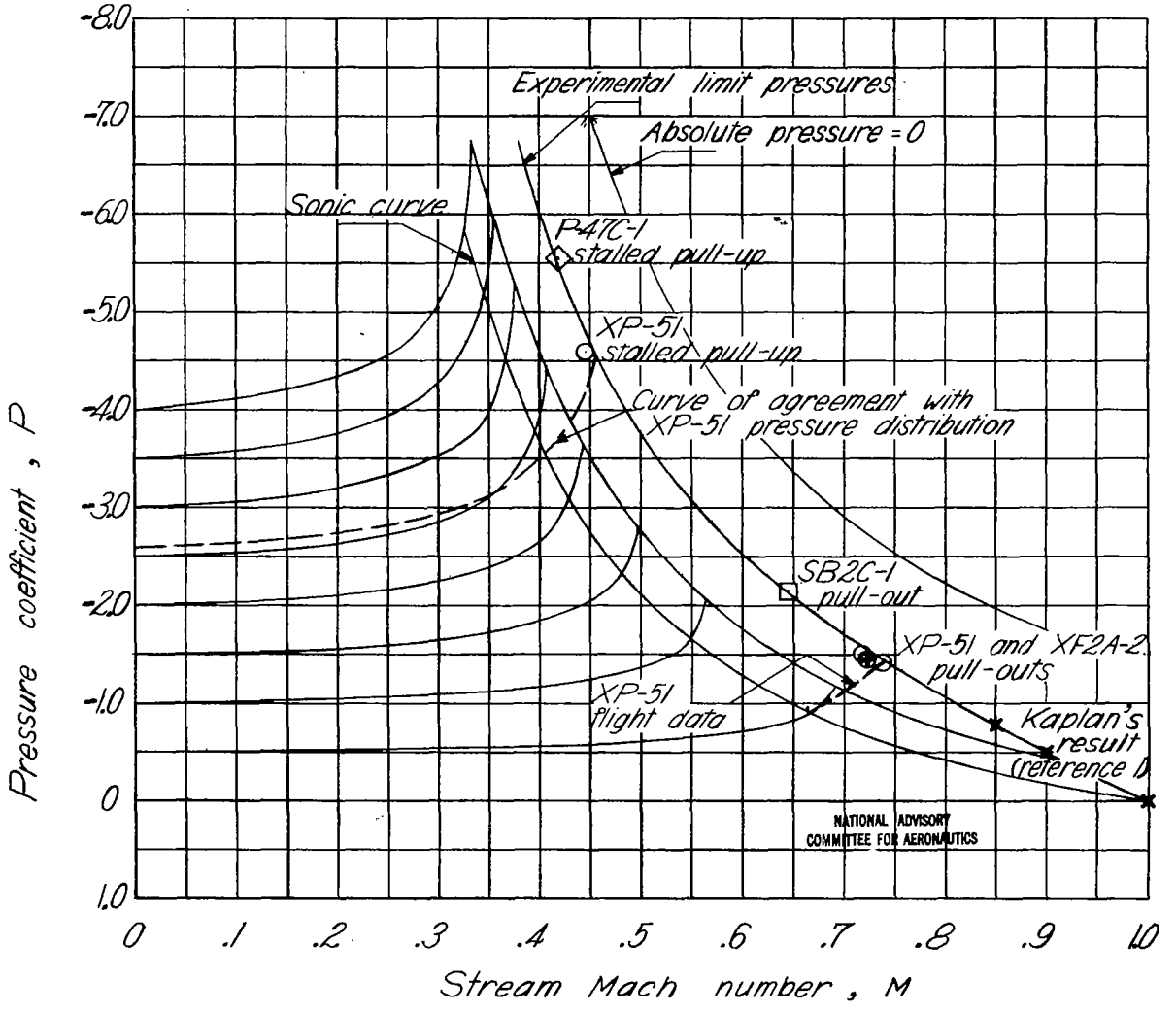

Figure 8.- Pressure coefficient against stream Mach number, according to Garrick and Kaplan, with experimental curve of limit pressure and other flight data.

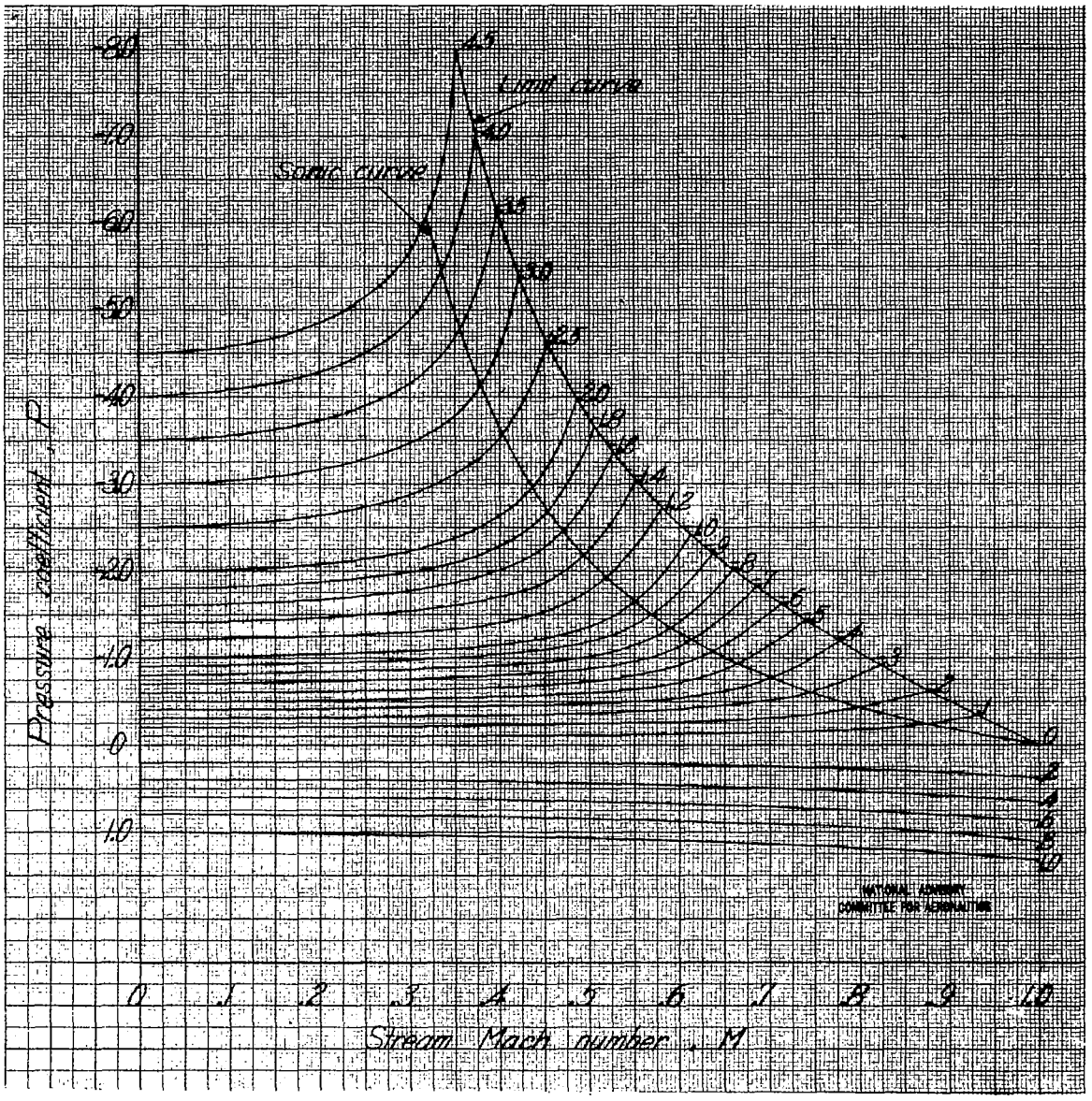

Figure 9.- Tentative working chart for solution of compressible flow of air to limit pressure.

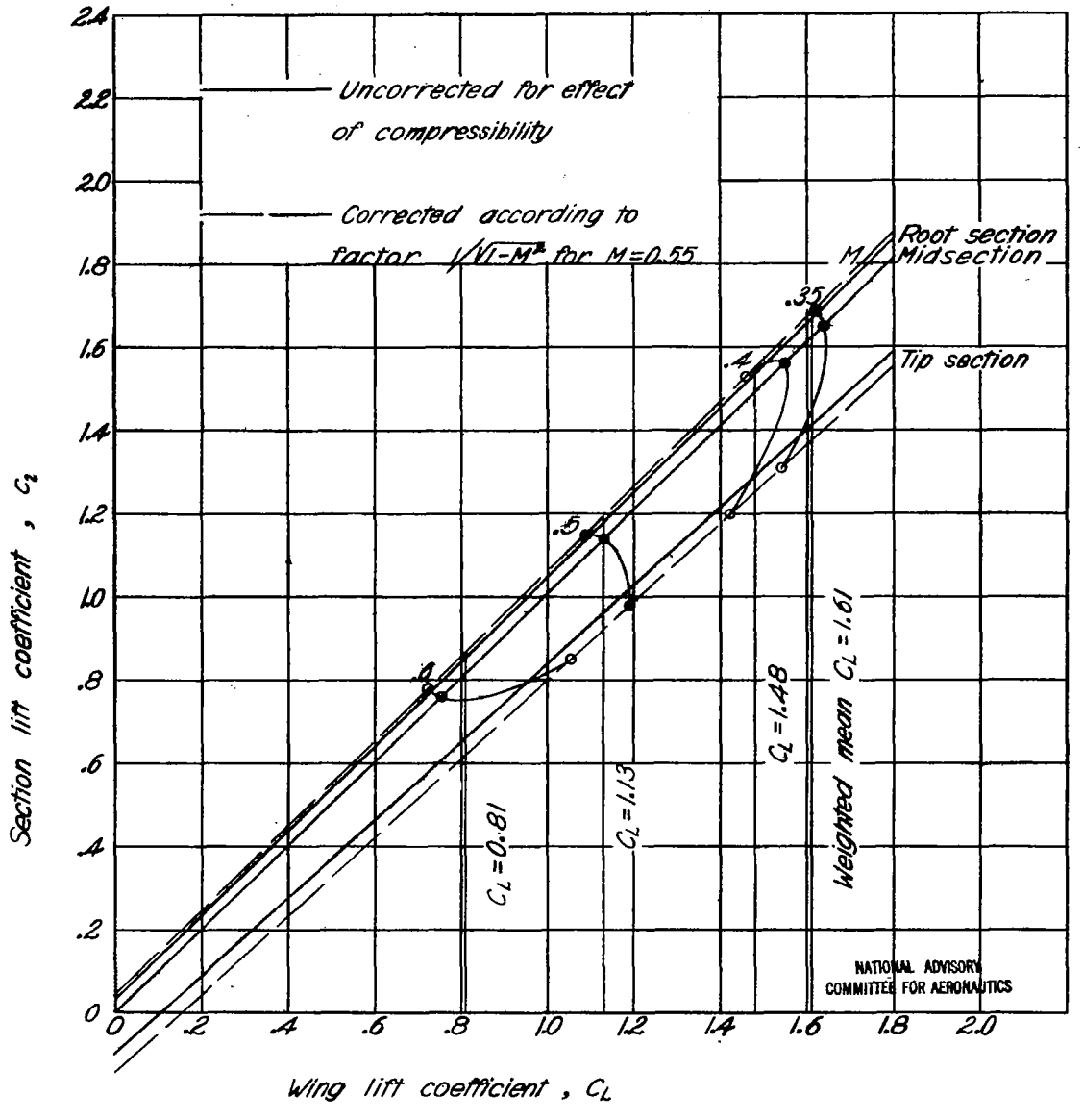

Figure 10.- Section lift coefficients corresponding to limit pressure at three spanwise stations on wing of P-47C-1 airplane and associated values of wing lift coefficient.

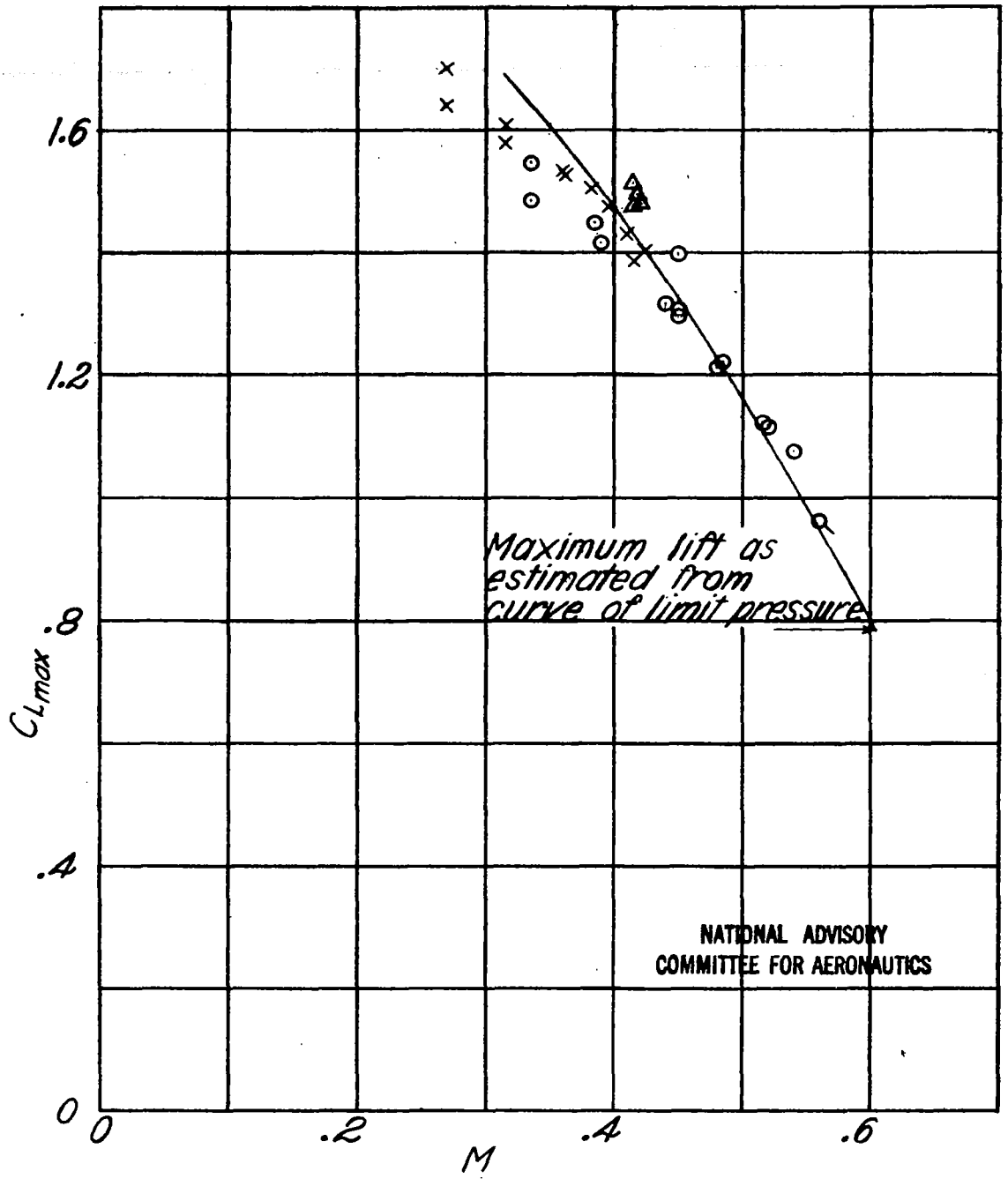

Figure 11.- Maximum lift coefficient of P-47C-1 airplane corrected for tail load and compared with wing maximum lift as estimated from curve of limit pressure.

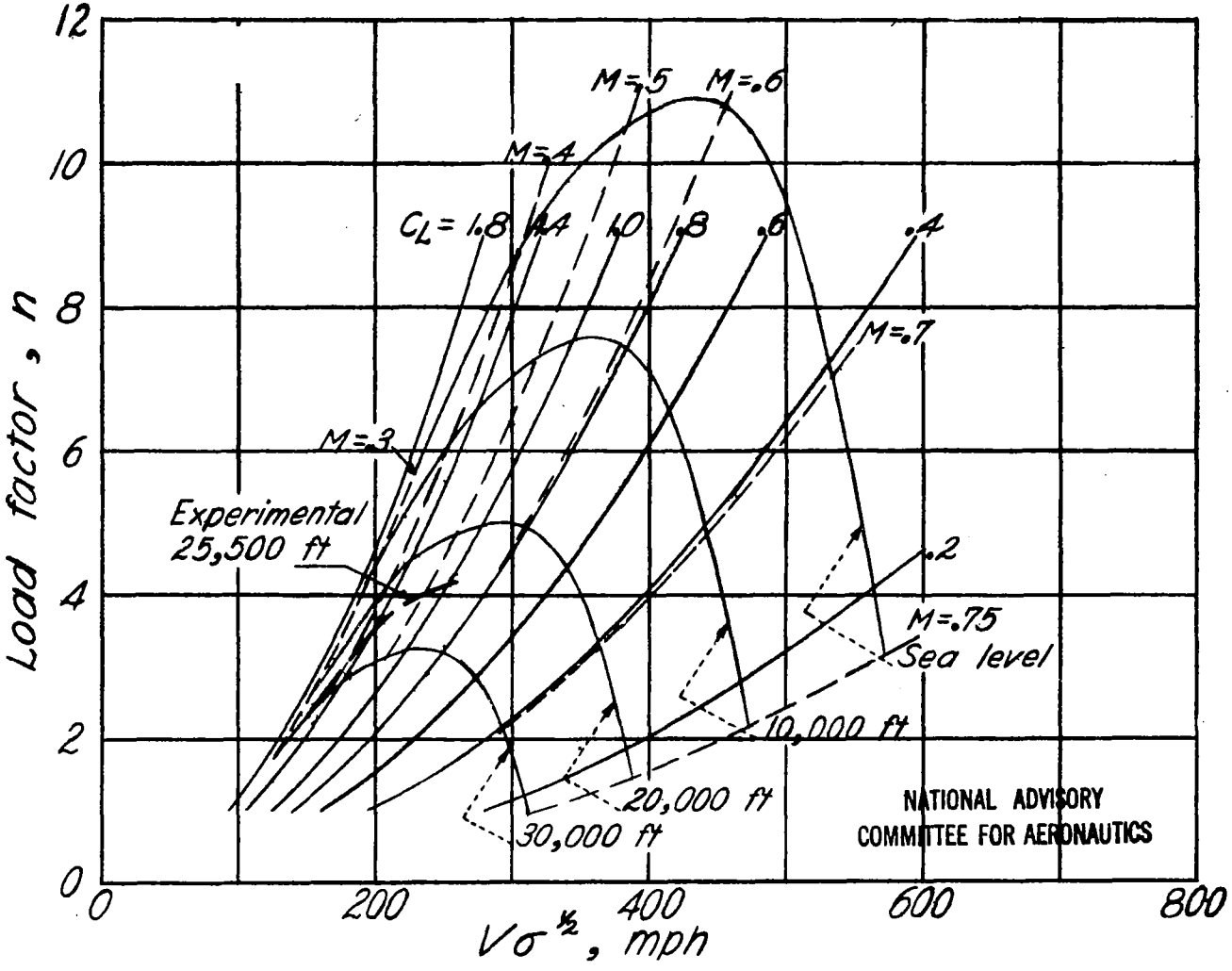

Figure 12.- V-n diagrams for P-47C-1 airplane showing boundaries defining burbling for a wing loading of 40 pounds per square foot.

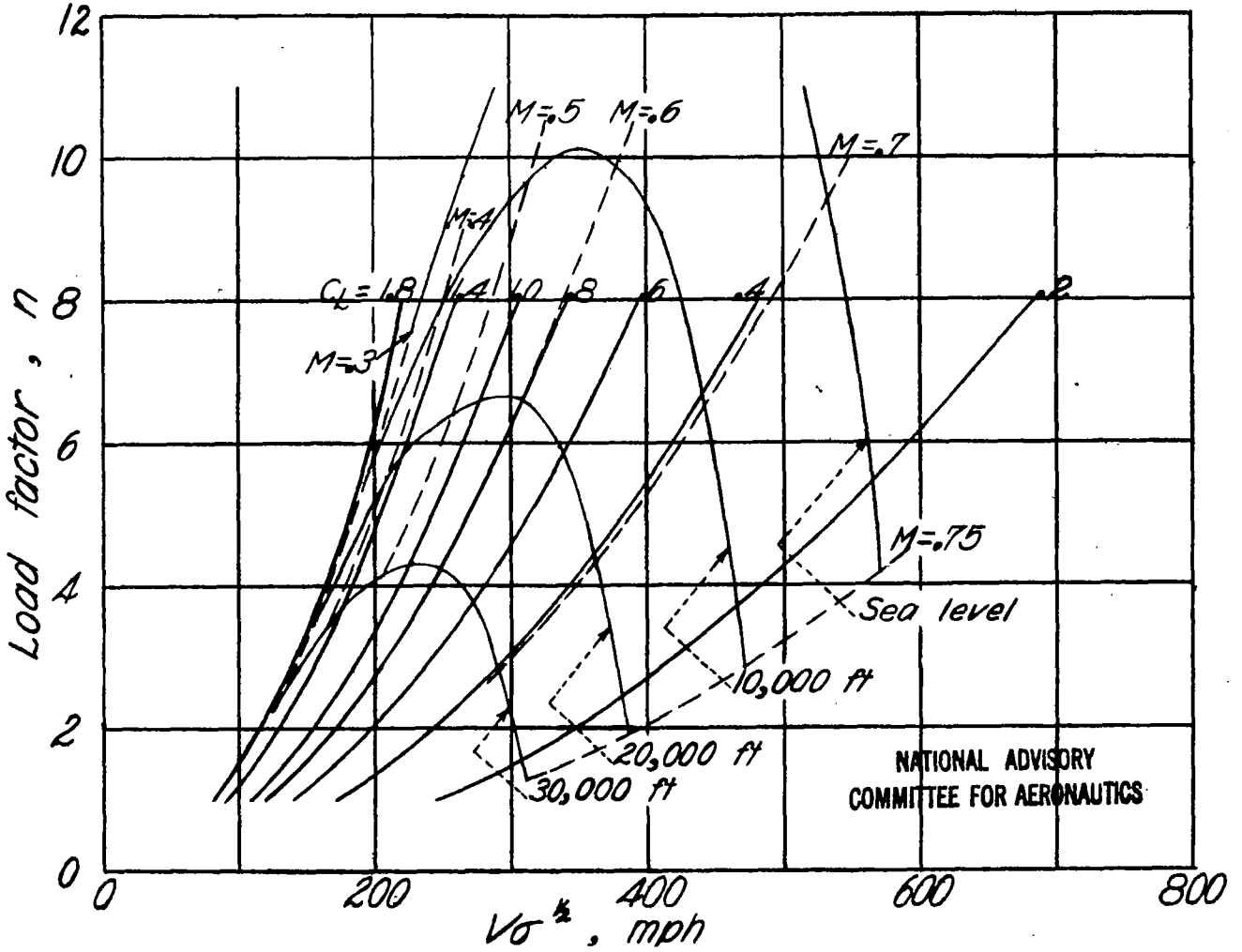

Figure 13.- V-n diagrams for P-47C-1 airplane showing boundaries defining burbling with wing loading reduced to 30 pounds per square foot.

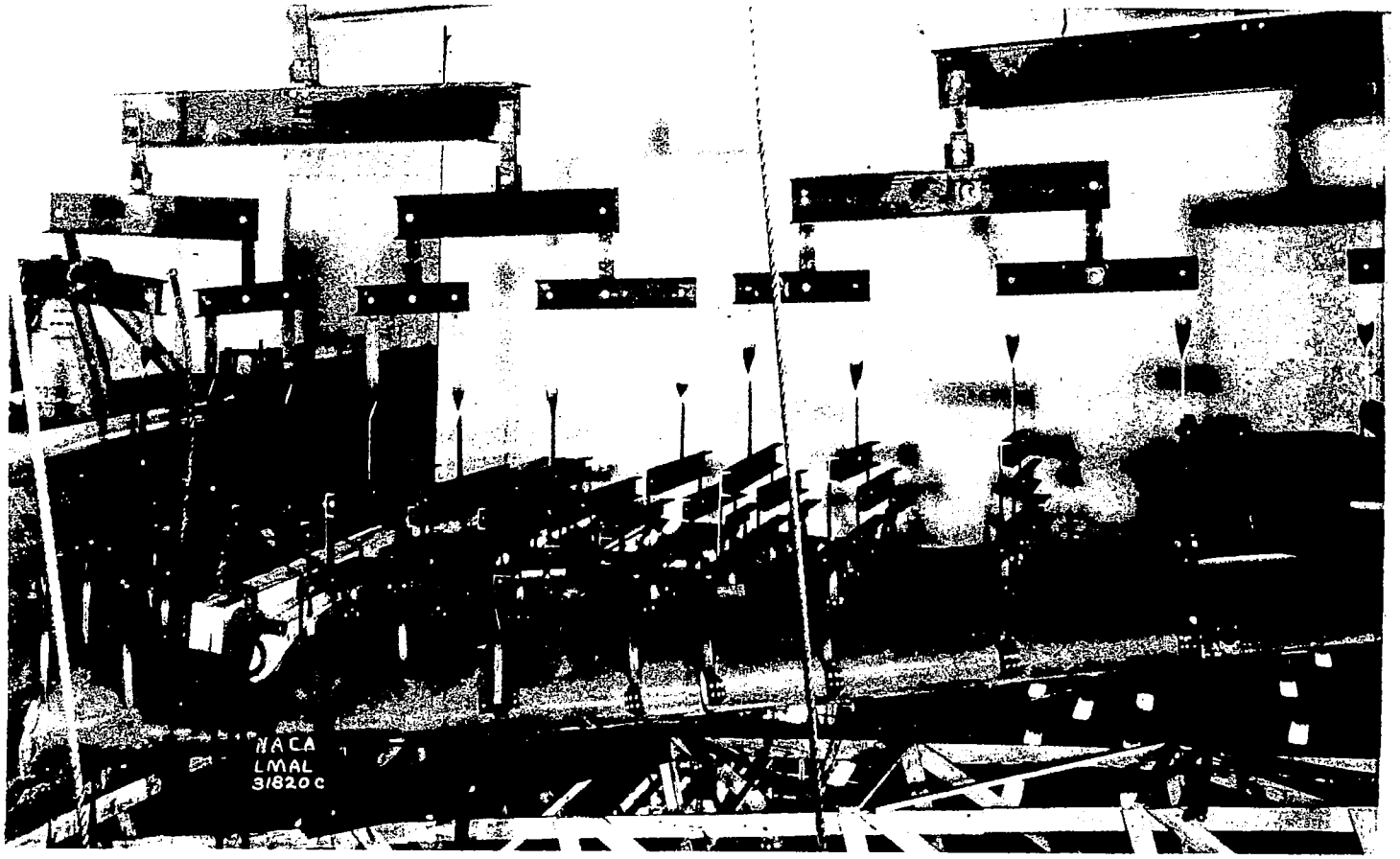

Figure 14.- Airplane wing under static test at a load factor of 8.

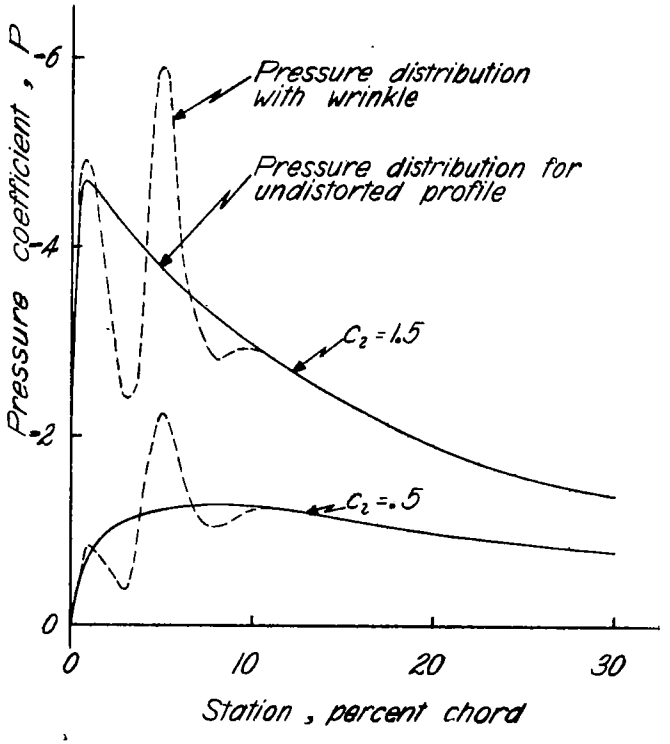

Figure 15.- Pressure distributions over upper surface of wing, showing effect of wrinkle, without correction for compressibility.

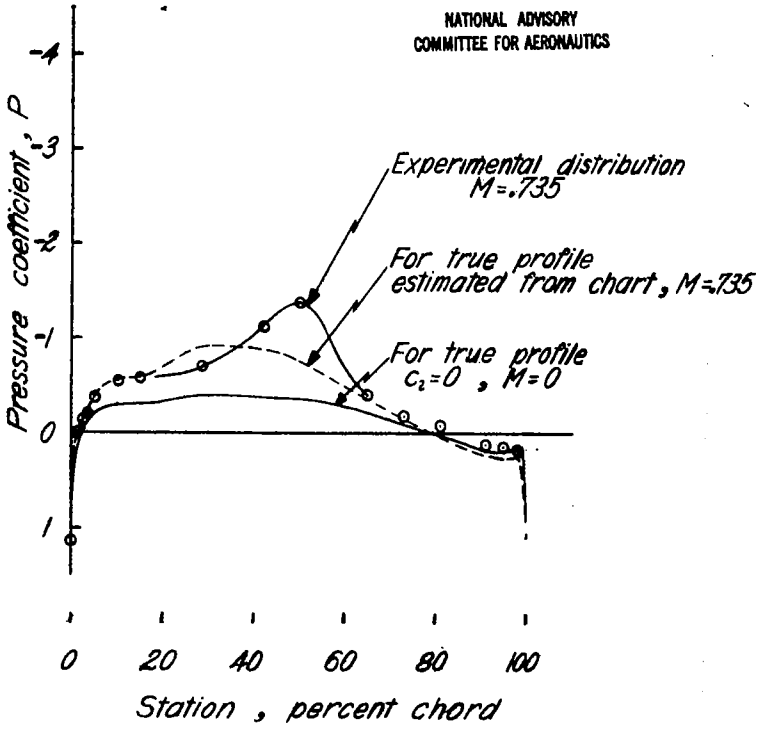

Figure 16.- Pressure distributions over upper surface of midsection of wing of XP-51 airplane.